Compressible Parabolized Stability Equation in Curvilinear Coordinate System and Integration

Bing Gao and S. O. Park*
Department of Aerospace Engineering,
Korea Advanced Institute of Science and Technology
373-1, Guseong-dong Yuseong-gu, Daejeon, 305-701, Korea

Abstract

Parabolized stability equations for compressible flows in general curvilinear coordinate system are derived to deal with a broad range of transition prediction problems on complex geometry. A highly accurate finite difference PSE code has been developed using an implicit marching procedure. Compressible and incompressible flat plate flow stability under two-dimensional and three-dimensional disturbances has been investigated to test the present code. Results of the present computation are found to be in good agreement with the multiple scale analysis and DNS data. Stability calculation results by the present PSE code for compressible boundary layer at Mach numbers ranging from 0.02 to 1.5 are also presented and are again seen to be as accurate as the spectral method.

Key Words : Parabolized stability equations, curvilinear coordinate system, compressible flows, and implicit marching procedure

Introduction

The subject of compressible boundary-layer stability has attracted a great deal of interest recently due to its importance in understanding the onset of transition in high-speed flows and providing some theoretical background for laminar flow control techniques. The objective of the present work is the development of an accurate and cost efficient code for analysizing the 2D or 3D boundary layer stability over complex geometries such as surface roughness elements, elliptic cones, or blunt cones at angle of attack.

Most investigations of compressible linear stability have employed linear stability theory approach (LST), which ignores the growth of the boundary layer and assumes locally parallel streamline. Its usefulness is limited by inaccuracies due to the parallel flow approximation. Another limitation is that the assumption of local parallel flow neglects the physical connection between the disturbances at different locations and introduces ambiguity in the calculation of amplitude factors. Different strategies have been suggested to overcome these deficiencies[1,2]. Another transition prediction tool is the direct numerical simulations (DNS) using the full Navier-Stokes equations. But it requires too much computer power. So far, DNS has been tried only for very simple geometries such as flat plate. A general consensus is that DNS is not appropriate for studying the transition over the realistic geometries[3].

* Professor, Aerospace Engineering Dept., KAIST
E-mail : sopark@kaist.ac.kr Tel : 82-42-869-3713 Fax : 82-42-869-3750

Since Herbert's introduction of parabolized stability equations (PSE) [4], it is gaining popularity for fluid dynamic stability research because of its ability to directly track disturbances along the marching direction with less computer power. However, most of the research efforts of PSE so far have been concerned with the stability of the flow past rather simple geometries, such as flat plate, infinite wing, and finite wing with smooth surface. How to utilize PSE for the flow stability over surface roughness elements or other complex geometry is still a challenging task at the present time. For the stability calculations on the flows associated with rather complex geometries, the PSE need be formulated in a general curvilinear coordinate system. The present work discusses the formulation of the PSE in curvilinear coordinate system and the development of the finite difference code.

Problem Formulations

2.1 Full disturbance equations in curvilinear coordinate system

Both the compressible linear stability equations (LST) and the parabolized stability equations (PSE) originate from the compressible Navier-Stokes equations. The three dimensional Navier-Stokes equations for the perfect gas are [5],

$$\rho^*[\frac{\partial u^*}{\partial t^*} + u^* \cdot \nabla u^*] = -\nabla p^* + \nabla \cdot [\lambda^*(\nabla \cdot u^*)I + \mu^*(\nabla u^* + \nabla u^{*tr}] \tag{1}$$

$$\frac{\partial \rho^*}{\partial t^*} + \nabla \cdot (\rho^* u^*) = 0 \tag{2}$$

$$\rho^* c_p^*[\frac{\partial T^*}{\partial t^*} + u^* \cdot \nabla T^*] = \nabla \cdot (k^* \nabla T^*) + \frac{\partial p^*}{\partial t^*} + u^* \cdot \nabla u^* + \Phi^* \tag{3}$$

$$p^* = \rho^* R^* T^* \tag{4}$$

where u^* is the velocity vector, ρ^* is the density, p^* is the pressure, T^* is the temperature, R^* is the gas constant, c_p^* is the specific heat at constant pressure, k^* is the thermal conductivity, μ^* is the first coefficient of viscosity, and λ^* is the second coefficient of viscosity. The viscous dissipation function, Φ^* is given as

$$\Phi^* = \lambda^*(\nabla \cdot u^*)^2 + \frac{\mu^*}{2}[\nabla u^* + \nabla u^{*tr}] \tag{5}$$

The superscript * denotes dimensional quantities. For non-dimensionalization of the governing equations, all the lengths are assumed scaled by a reference length $L^* = \sqrt{\nu_\infty^* x_0^* / u_\infty^*}$, velocity by u_∞^*, density by ρ_∞^*, pressure by $\rho_\infty^* u_\infty^{*2}$, and time by L^*/u_∞^* and other variables by their corresponding boundary layer edge values. The instantaneous non-dimensional values of velocities, u, v, w, pressure p, temperature T, density ρ, may be represented as the sum of a mean and fluctuation quantity, i.e.,

$$\begin{aligned} u &= \overline{U} + \tilde{u} \quad v = \overline{V} + \tilde{v} \quad w = \overline{W} + \tilde{w} \\ p &= \overline{P} + \tilde{p} \quad T = \overline{T} + \tilde{T} \quad \rho = \overline{\rho} + \tilde{\rho} \\ \mu &= \overline{\mu} + \tilde{\mu} \quad \lambda = \overline{\lambda} + \tilde{\lambda} \quad k = \overline{k} + \tilde{k} \end{aligned} \tag{6}$$

Substitution of (6) into the non-dimensional form of governing equations yields the linearized full perturbation equation in Cartesian coordinate system,

$$\Gamma \frac{\partial \phi}{\partial t} + A \frac{\partial \phi}{\partial x} + B \frac{\partial \phi}{\partial y} + C \frac{\partial \phi}{\partial z} + D\phi = V_{xx} \frac{\partial^2 \phi}{\partial x^2} + V_{yy} \frac{\partial^2 \phi}{\partial y^2} + V_{zz} \frac{\partial^2 \phi}{\partial z^2} + V_{yz} \frac{\partial^2 \phi}{\partial y \partial z} + V_{xz} \frac{\partial^2 \phi}{\partial x \partial z} + V_{xy} \frac{\partial^2 \phi}{\partial x \partial y} \tag{7}$$

where ϕ contains the disturbance vector and is defined as $\phi = [\tilde{p}, \tilde{u}, \tilde{v}, \tilde{w}, \tilde{T}]^T$, and the coefficients are composed of mean flow quantities, which are given in appendix A.

The original PSE is based on the assumption that the velocity profiles, wavelengths, and growth rates change slowly in the streamwise direction. This assumption can hardly be satisfied for the flows where streamwise variation of mean flow is significant such as the flow over a hump or other complex geometries. To deal with this situation, it would be more convenient to write the PSE in curvilinear coordinate system. Let us consider a $\xi - \eta - \zeta$ system with

$$\xi = \xi(x, y, z) \; ; \; \eta = \eta(x, y, z) \; ; \; \zeta = \zeta(x, y, z) \tag{8}$$

where ξ, η, ζ are streamwise, normal, and spanwise direction coordinates, respectively. Substitution of (8) into (7) yields the following full disturbance equations in curvilinear coordinate system,

$$\overline{\Gamma} \frac{\partial \phi}{\partial t} + \overline{A} \frac{\partial \phi}{\partial \xi} + \overline{B} \frac{\partial \phi}{\partial \eta} + \overline{C} \frac{\partial \phi}{\partial \zeta} + \overline{D}\phi = \overline{V}_{\xi\xi} \frac{\partial^2 \phi}{\partial \xi^2} + \overline{V}_{\eta\eta} \frac{\partial^2 \phi}{\partial \eta^2} + \overline{V}_{\zeta\zeta} \frac{\partial^2 \phi}{\partial \zeta^2} + \overline{V}_{\xi\eta} \frac{\partial^2 \phi}{\partial \xi \partial \eta} + \overline{V}_{\xi\zeta} \frac{\partial^2 \phi}{\partial \xi \partial \zeta} + \overline{V}_{\eta\zeta} \frac{\partial^2 \phi}{\partial \eta \partial \zeta} \tag{9}$$

where the coefficients with overbar are provided in detail in the Appendix B.

2.2 Full-3D linearized PSE

Direct solution of the disturbance equations (9) is referred to as the direct numerical simulation (DNS) method. DNS requires a significant amount of computational power even for a very simple case. Naturally a more efficient approximate method is desirable. The disturbance equations are elliptic in the streamwise direction. We can parabolize the disturbance equations and make the marching solution feasible by neglecting the viscous diffusion terms along the streamwise direction similarly to the parabolized Navier-Stokes equations (PNS). But direct application of the parabolizing procedure used in the PNS approach for mean flow computations to the disturbance equations would not capture the flow physics due to the suppression of the wave propagation along the left-running characteristics[6]. Herbert and Morkovin[7] also commented that the relatively short wavelength of instability waves causes streamwise changes too large to be neglected. Chang and Malik[6] further pointed out that the disturbances are essentially unsteady waves propagating across the whole boundary layer and the amplitudes of these waves reach their maxima near the critical layer located between the wall and the boundary layer edge. These instability waves undergo a "fast-oscillation" (phase change) as they evolve along the flow direction. Thus the disturbances can be decomposed into a fast-oscillatory wave part and a slowly varying shape function. By this arrangement, the ellipticity for the wave part is kept while parabolizing the governing equations for the shape function. The disturbance is expressed as

$$\phi(\xi, \eta, \zeta, t) = \psi(\xi, \eta, \zeta) \exp\left[i\theta(\xi, \zeta, t)\right] \tag{10}$$

where ψ is the shape function and is defined as $\psi = (\hat{p}, \hat{u}, \hat{v}, \hat{w}, \hat{T})^T$, θ is a phase function. It is assumed that the disturbance vector ϕ has a frequency ω and a spanwise wave number β and a streamwise wave number α , thus

$$\frac{\partial \theta}{\partial t} = -\omega \ ; \ \alpha(\xi,\zeta) = \frac{\partial \theta}{\partial \xi} ; \ \ \beta(\xi,\zeta) = \frac{\partial \theta}{\partial \zeta} \tag{11}$$

From Eq.(11), we see that the wave number must satisfy the irrotationality condition [8].

$$\frac{\partial \alpha}{\partial \zeta} = \frac{\partial \beta}{\partial \xi} = \frac{\partial^2 \theta}{\partial \xi \partial \zeta} \tag{12}$$

Substitution of Eqs. (10) and (11) into Eq. (9) yields

$$\begin{aligned} &\widetilde{D}\psi + \widetilde{A}\frac{\partial \psi}{\partial \xi} + \widetilde{B}\frac{\partial \psi}{\partial \eta} + \widetilde{C}\frac{\partial \psi}{\partial \zeta} \\ &= \widetilde{V}_{\xi\xi}\frac{\partial^2 \psi}{\partial \xi^2} + \widetilde{V}_{\eta\eta}\frac{\partial^2 \psi}{\partial \eta^2} + \widetilde{V}_{\zeta\zeta}\frac{\partial^2 \psi}{\partial \zeta^2} + \widetilde{V}_{\xi\eta}\frac{\partial^2 \psi}{\partial \xi \partial \eta} + \widetilde{V}_{\xi\zeta}\frac{\partial^2 \psi}{\partial \xi \partial \zeta} + \widetilde{V}_{\eta\zeta}\frac{\partial^2 \psi}{\partial \eta \partial \zeta} \end{aligned} \tag{13}$$

where

$$\begin{aligned} &\widetilde{D} = -i\omega\overline{\Gamma} + i\alpha\overline{A} + i\beta\overline{C} + \overline{D} + \overline{V}_{\xi\xi}\alpha^2 + \overline{V}_{\xi\zeta}\alpha\beta + \overline{V}_{\zeta\zeta}\beta^2 \\ &-i(\overline{V}_{\xi\xi}\frac{\partial \alpha}{\partial \xi} + \overline{V}_{\xi\zeta}\frac{\partial \alpha}{\partial \zeta} + \overline{V}_{\zeta\zeta}\frac{\partial \beta}{\partial \zeta}) \\ &\widetilde{A} = \overline{A} - 2i\alpha\overline{V}_{\xi\xi} - i\beta\overline{V}_{\xi\zeta} \\ &\widetilde{B} = \overline{B} - i\alpha\overline{V}_{\xi\eta} - i\beta\overline{V}_{\eta\zeta} \\ &\widetilde{C} = \overline{C} - i\alpha\overline{V}_{\xi\zeta} - 2i\beta\overline{V}_{\zeta\zeta} \\ &\widetilde{V}_{\eta\eta} = \overline{V}_{\eta\eta}; \widetilde{V}_{\xi\xi} = V_{\xi\xi}; \widetilde{V}_{\zeta\zeta} = \overline{V}_{\zeta\zeta}; \widetilde{V}_{\xi\eta} = \overline{V}_{\xi\eta}; \widetilde{V}_{\xi\zeta} = \overline{V}_{\xi\zeta}; \widetilde{V}_{\eta\zeta} = \overline{V}_{\eta\zeta} \end{aligned} \tag{14}$$

It is noted that the matrices $\widetilde{A}, \widetilde{B}, \widetilde{C}, \widetilde{D}$ have contributions from both inviscid and viscous terms, and thus contain terms of order one and of order $1/R_0$ (R_0 is the reference Reynolds number $R_0 = u_\infty^* L^* / \nu_\infty^*$); while matrices $\widetilde{V}_{\xi\xi}, \widetilde{V}_{\xi\eta}, \widetilde{V}_{\xi\zeta}, \widetilde{V}_{\eta\zeta}, \widetilde{V}_{\eta\eta}, \widetilde{V}_{\zeta\zeta}$ are solely due to viscous diffusion and are of order $1/R_0$. The shape function is assumed to be changed slowly along the streamwise and spanwise directions. Its derivatives along both directions are assumed to be of order $1/R_0$. After neglecting all the terms which are of order $1/R_0^2$, the full 3D PSE can be obtained as follows.

$$\widetilde{D}\psi + \widetilde{A}\frac{\partial \psi}{\partial \xi} + \widetilde{B}\frac{\partial \psi}{\partial \eta} + \widetilde{C}\frac{\partial \psi}{\partial \zeta} = \widetilde{V}_{\eta\eta}\frac{\partial^2 \psi}{\partial \eta^2} \tag{15}$$

2.3 Quasi-3D linearized PSE equations

For the stability analysis of two dimensional mean flows, it is sufficient to consider only quasi−3D disturbance whose spanwise wave number is constant. Then the disturbance vector ϕ can be expressed as

$$\phi(\xi,\eta,\zeta,t) = \psi(\xi,\eta)\exp[i\theta(\xi,\zeta,t)] \tag{16}$$

where

$$\frac{\partial \theta}{\partial t} = -\omega \ ; \ \frac{\partial \theta}{\partial \xi} = \alpha(\xi); \ \ \frac{\partial \theta}{\partial \zeta} = \beta \tag{17}$$

The streamwise wave number α is a function only of ξ; the spanwise wave number β is kept constant as disturbances propagate downstream. In this case, Eq.(15) is further simplified to

$$\widetilde{D}\psi + \widetilde{A}\frac{\partial \psi}{\partial \xi} + \widetilde{B}\frac{\partial \psi}{\partial \eta} = \widetilde{V}_{\eta\eta}\frac{\partial^2 \psi}{\partial \eta^2} \tag{18}$$

where

$$\begin{aligned}
\widetilde{D} &= -i\omega\overline{\Gamma} + i\alpha\overline{A} + i\beta\overline{C} + \overline{D} + \overline{V}_{\xi\xi}\alpha^2 + \overline{V}_{\xi\zeta}\alpha\beta + \overline{V}_{\zeta\zeta}\beta^2 - i\overline{V}_{\xi\xi}\frac{d\alpha}{d\xi} \\
\widetilde{A} &= \overline{A} - 2i\alpha\overline{V}_{\xi\xi} - i\beta\overline{V}_{\xi\zeta} \\
\widetilde{B} &= \overline{B} - i\alpha\overline{V}_{\xi\eta} - i\beta\overline{V}_{\eta\zeta} \\
\widetilde{V}_{\eta\eta} &= \overline{V}_{\eta\eta}
\end{aligned} \tag{19}$$

2.4 Boundary conditions

The solution of Eq. (15) or Eq. (18) requires proper boundary conditions in the wall-normal direction. We apply the following homogeneous Dirichlet conditions.

$$\hat{u} = 0, \hat{v} = 0, \hat{w} = 0, \hat{T} = 0 \quad \text{at } \eta = 0 \tag{20}$$

$$\hat{u} = 0, \hat{v} = 0, \hat{w} = 0, \hat{T} = 0 \quad \text{at } \eta \to \infty \tag{21}$$

The temperature boundary condition at the wall is reasonable because the disturbance's frequency is much greater compared to the thermal response time of the wall [9].

2.5 Normalization conditions

The partition of ϕ into ψ and θ in Eqs. (10) and (16) bears ambiguity since both ψ and θ depend on ξ. That is, part of the exponential factor can be included in ψ without any change in the form of the partition. To overcome this ambiguity, an additional normalization equation is required. The hypothesis of PSE is that the shape function ψ changes slowly and its derivative is of order $1/R_0$ in both the streamwise and the spanwise directions. Herbert[10] suggested normalization conditions in Cartesian coordinate system to make that hypothesis feasible. Here we follow Herbert and give the same normalization conditions in curvilinear coordinate system as follows.
For full 3D disturbance,

$$\int_\Omega (\hat{u}^\dagger \frac{\partial \hat{u}}{\partial \xi} + \hat{v}^\dagger \frac{\partial \hat{v}}{\partial \xi} + \hat{w}^\dagger \frac{\partial \hat{w}}{\partial \xi}) d\eta = 0 \,, \quad \int_\Omega (\hat{u}^\dagger \frac{\partial \hat{u}}{\partial \xi} + \hat{v}^\dagger \frac{\partial \hat{v}}{\partial \xi} + \hat{w}^\dagger \frac{\partial \hat{w}}{\partial \xi}) d\eta = 0 \tag{22}$$

For quasi-3D disturbance,

$$\int_\Omega (\hat{u}^\dagger \frac{\partial \hat{u}}{\partial \xi} + \hat{v}^\dagger \frac{\partial \hat{v}}{\partial \xi} + \hat{w}^\dagger \frac{\partial \hat{w}}{\partial \xi}) d\eta = 0 \tag{23}$$

This choice makes the total kinetic energy $E = \int_\Omega (|\hat{u}|^2 + |\hat{v}|^2 + |\hat{w}|^2) d\eta$ of the shape functions independent of ξ or ζ. The growth of the disturbance energy is absorbed into the phase function θ.

2.6 Measure of physical growth rate

The growth rate of certain physical quantity Q is defined as the logarithmic derivative

$$\overline{\gamma} = real(\frac{1}{Q}\frac{\partial Q}{\partial x}) = real\left[\frac{1}{Q}(\frac{\partial Q}{\partial \xi}\xi_x + \frac{\partial Q}{\partial \eta}\eta_x + \frac{\partial Q}{\partial \zeta}\zeta_x)\right] \tag{24}$$

where the division by Q renders the result independent of the magnitude of Q. When we take Q as ϕ of Eq. (16), we have

$$Q(\xi,\eta,\zeta,t) = \widehat{Q}(\xi,\eta)\exp[i\theta(\xi,\zeta,t)] \tag{25}$$

and

$$\overline{\gamma} = real\left[(\frac{1}{\widehat{Q}}\frac{\partial \widehat{Q}}{\partial \xi} + i\alpha)\xi_x + \frac{1}{\widehat{Q}}\frac{\partial \widehat{Q}}{\partial \eta}\eta_x + i\beta\zeta_x\right] \tag{26}$$

To make the growth rate more specific, we follow Malik[11] and define the growth rate as

$$\overline{\gamma} = real\left\{(\frac{\int_0^\infty \hat{q}_n^\dagger \frac{\partial \hat{q}_n}{\partial \xi}d\eta}{\int_0^\infty |\hat{q}_n|^2 d\eta} + i\alpha)\xi_x + (\frac{\int_0^\infty \hat{q}_n^\dagger \frac{\partial \hat{q}_n}{\partial \eta}d\eta}{\int_0^\infty |\hat{q}_n|^2 d\eta})\eta_x + i\beta\zeta_x\right\} \tag{27}$$

where $\hat{q}_n = (\hat{u},\hat{v},\hat{w})^T$

The definition of Eq. (27) is yet ambiguous since it is affected by the choice of position in y direction. We thus choose the maximum growth rate as the physical growth rate, that is,

$$\overline{\gamma} = \max_y real\left\{(\frac{\int_0^\infty \hat{q}_n^\dagger \frac{\partial \hat{q}_n}{\partial \xi}d\eta}{\int_0^\infty |\hat{q}_n|^2 d\eta} + i\alpha)\xi_x + (\frac{\int_0^\infty \hat{q}_n^\dagger \frac{\partial \hat{q}_n}{\partial \eta}d\eta}{\int_0^\infty |\hat{q}_n|^2 d\eta})\eta_x + i\beta\zeta_x\right\} \tag{28}$$

Numerical Methods

So far, most of researchers have solved the PSE by spectral method for accuracy. However, the spectral method is not easy to apply for the flows over complex geometries. Therefore, a high-order finite difference method is chosen for the present work for the solution of PSE in general curvilinear coordinate system.

The determining factor in choosing the streamwise marching scheme is stability. Thus implicit backward Euler method is usually adopted for marching. In the wall normal direction, fourth-order finite difference method is employed[5] and one-side difference which does not involve the wall points is used to approximate the first derivative of pressure.

More specifically the discretization form of Eq. (18) can be written as follows, where i,j denotes the grid index in the streamwise and normal direction; JM denotes the maximum grid number in the normal direction.

For $j = 2$

$$\begin{aligned}&\widetilde{D}\psi_{ij} + \widetilde{A}\frac{\psi_{ij} - \psi_{i-1j}}{\Delta\xi} + m_1\widetilde{B}\frac{-3\psi_{ij-1} - 10\psi_{ij} + 18\psi_{ij+1} - 6\psi_{ij+2} + \psi_{ij+3}}{12\Delta\eta}\\ &+ m_2\widetilde{B}\frac{-25\psi_{ij} + 48\psi_{ij+1} - 36\psi_{ij+2} + 16\psi_{ij+3} - 3\psi_{ij+4}}{12\Delta\eta}\\ &= \widetilde{V}_{\eta\eta}\frac{10\psi_{ij-1} - 15\psi_{ij} - 4\psi_{ij+1} + 14\psi_{ij+2} - 6\psi_{ij+3} + \psi_{ij+4}}{12\Delta\eta^2}\end{aligned} \tag{29}$$

For $j = 3$

$$\begin{aligned}&\widetilde{D}\psi_{ij} + \widetilde{A}\frac{\psi_{ij} - \psi_{i-1\,j}}{\Delta\xi} + m_1\widetilde{B}\frac{\psi_{ij-2} - 8\psi_{ij-1} + 8\psi_{ij+1} - \psi_{ij+2}}{12\Delta\eta}\\&+ m_2\widetilde{B}\frac{-3\psi_{ij-1} - 10\psi_{ij} + 18\psi_{ij+1} - 6\psi_{ij+2} + \psi_{ij+3}}{12\Delta\eta}\\&= \widetilde{V}_{\eta\eta}\frac{-\psi_{ij-2} + 16\psi_{ij-1} - 30\psi_{ij} + 16\psi_{ij+1} - \psi_{ij+2}}{12\Delta\eta^2}\end{aligned} \tag{30}$$

For $3 < j < JM - 2$

$$\begin{aligned}&\widetilde{D}\psi_{ij} + \widetilde{A}\frac{\psi_{ij} - \psi_{i-1\,j}}{\Delta\xi} + \widetilde{B}\frac{\psi_{ij-2} - 8\psi_{ij-1} + 8\psi_{ij+1} - \psi_{ij+2}}{12\Delta\eta}\\&= \widetilde{V}_{\eta\eta}\frac{-\psi_{ij-2} + 16\psi_{ij-1} - 30\psi_{ij} + 16\psi_{ij+1} - \psi_{ij+2}}{12\Delta\eta^2}\end{aligned} \tag{31}$$

For $j = JM - 2$

$$\begin{aligned}&\widetilde{D}\psi_{ij} + \widetilde{A}\frac{\psi_{ij} - \psi_{i-1\,j}}{\Delta\xi} + m_1\widetilde{B}\frac{\psi_{ij-2} - 8\psi_{ij-1} + 8\psi_{ij+1} - \psi_{ij+2}}{12\Delta\eta}\\&+ m_2\widetilde{B}\frac{-\psi_{ij-3} + 6\psi_{ij-2} - 18\psi_{ij-1} + 10\psi_{ij} + 3\psi_{ij+1}}{12\Delta\eta}\\&= \widetilde{V}_{\eta\eta}\frac{-\psi_{ij-2} + 16\psi_{ij-1} - 30\psi_{ij} + 16\psi_{ij+1} - \psi_{ij+2}}{12\Delta\eta^2}\end{aligned} \tag{32}$$

For $j = JM - 1$

$$\begin{aligned}&\widetilde{D}\psi_{ij} + \widetilde{A}\frac{\psi_{ij} - \psi_{i-1\,j}}{\Delta\xi} + m_1\widetilde{B}\frac{-\psi_{ij-3} + 6\psi_{ij-2} - 18\psi_{ij-1} + 10\psi_{ij} + 3\psi_{ij+1}}{12\Delta\eta}\\&+ m_2\widetilde{B}\frac{3\psi_{ij-4} - 16\psi_{ij-3} + 36\psi_{ij-2} - 48\psi_{ij-1} + 25\psi_{ij}}{12\Delta\eta}\\&= \widetilde{V}_{\eta\eta}\frac{\psi_{ij-4} - 6\psi_{ij-3} + 14\psi_{ij-2} - 4\psi_{ij-1} - 15\psi_{ij} + 10\psi_{ij+1}}{12\Delta\eta^2}\end{aligned} \tag{33}$$

where $m_1 = 1, m_2 = 0$ for component $\hat{u}, \hat{v}, \hat{w}, \hat{T}$; $m_1 = 0, m_2 = 1$ for component $\hat{p}$. Eqs. (29)– (33) can be rearranged into matrix form as follows.

$$\begin{bmatrix}
\underline{C}_{i,2} & \underline{D}_{i,2} & \underline{E}_{i,2} & \underline{F}_{i,2} & \underline{G}_{i,2} & & & & & & \\
\underline{B}_{i,3} & \underline{C}_{i,3} & \underline{D}_{i,3} & \underline{E}_{i,3} & \underline{F}_{i,3} & & & & & & \\
\underline{A}_{i,4} & \underline{B}_{i,4} & \underline{C}_{i,4} & \underline{D}_{i,4} & \underline{E}_{i,4} & & & & & & \\
 & \underline{A}_{i,5} & \underline{B}_{i,5} & \underline{C}_{i,5} & \underline{D}_{i,5} & \underline{E}_{i,5} & & & & & \\
 & & \underline{A}_{i,6} & \underline{B}_{i,6} & \underline{C}_{i,6} & \underline{D}_{i,6} & \underline{E}_{i,6} & & & & \\
 & & & & \cdot & \cdot & \cdot & \cdot & \cdot & & \\
 & & & & \underline{A}_{i,JM-4} & \underline{B}_{i,JM-4} & \underline{C}_{i,JM-4} & \underline{D}_{i,JM-4} & \underline{E}_{i,JM-4} & & \\
 & & & & & \underline{A}_{i,JM-3} & \underline{B}_{i,JM-3} & \underline{C}_{i,JM-3} & \underline{D}_{i,JM-3} & \underline{E}_{i,JM-3} & \\
 & & & & & \underline{AA}_{i,JM-2} & \underline{A}_{i,JM-2} & \underline{B}_{i,JM-2} & \underline{C}_{i,JM-2} & \underline{D}_{i,JM-2} & \\
 & & & & & \underline{AA}_{i,JM-1} & \underline{AB}_{i,JM-1} & \underline{A}_{i,JM-1} & \underline{B}_{i,JM-1} & \underline{C}_{i,JM-1}
\end{bmatrix}
\begin{pmatrix}
\psi_{i,2} \\ \psi_{i,3} \\ \psi_{i,4} \\ \psi_{i,5} \\ \psi_{i,6} \\ \cdot \\ \psi_{i,JM-4} \\ \psi_{i,JM-3} \\ \psi_{i,JM-2} \\ \psi_{i,JM-1}
\end{pmatrix} =
\begin{pmatrix}
R_{i,2} \\ R_{i,3} \\ R_{i,4} \\ R_{i,5} \\ R_{i,6} \\ \cdot \\ R_{i,JM-4} \\ R_{i,JM-3} \\ R_{i,JM-2} \\ R_{i,JM-1}
\end{pmatrix} \tag{34}$$

The PSE is nonlinear because the coefficients include the unknown quantity α. An iterative procedure for α based on Eq. (23) is given as follows:

$$\alpha^{N} = \alpha^{O} - i\left[\int_0^{\infty} \hat{q}_n^{\dagger} \frac{\partial \hat{q}_n}{\partial \xi} d\eta \Big/ \int_0^{\infty} \left|\hat{q}_n\right|^2 d\eta\right] \tag{35}$$

where $\hat{q}_n = (\hat{u}, \hat{v}, \hat{w})$, The superscript N and O indicate new value and old values. Eq. (35) represents a two-dimensional iterative map whose convergence is not proved. However, Malik[11] has shown that this iterative procedure is a satisfactory approach for computing α.

The iteration procedure is summarized below.

1. Solve for ψ_{i+1} while evaluating matrices $\tilde{D}, \tilde{A}, \tilde{B}, \tilde{V}_{\eta\eta}$ at $i+1$ station
2. Update α_{i+1}^{N} using new ψ_{i+1} based on Eq. (35).
3. Check if $\alpha_{i+1}^{N} - \alpha_{i+1}^{O} < \varepsilon$. If yes, proceed to next station; otherwise go to step 1

Initial conditions

The PSE is a set of parabolic equations which require initial conditions at the starting location. To simulate the realistic conditions, the solution of PSE should be initiated by taking into account the free-stream disturbances. We initiate our PSE solution at some location ahead of the neutral curve where a parallel local approximation to the PSE is used to obtain the initial conditions. Under the assumption of parallel streamline ($\partial\psi/\partial\xi = 0$), Eq. (18) can be written as

$$\tilde{D}\psi + \tilde{B}\frac{\partial\psi}{\partial\eta} = \tilde{V}_{\eta\eta}\frac{\partial^2\psi}{\partial\eta^2} \tag{36}$$

The elements of matrices $\tilde{D}, \tilde{B}$ and $\tilde{V}_{\eta\eta}$ are evaluated by assuming parallel mean flows ($V=0$, $d\alpha/d\xi = 0$). Eq. (36) in conjunction with homogeneous boundary conditions constitutes an eigenvalue problem which leads to the dispersion relation

$$\alpha = \alpha(\omega, \beta) \tag{37}$$

Eq.(19) with parallel flow assumption can be cast into

$$\begin{aligned}
\tilde{D} &= \alpha^2\tilde{D}_2 + \alpha\tilde{D}_1 + \tilde{D}_0 \\
\tilde{B} &= \alpha^2\tilde{B}_2 + \alpha\tilde{B}_1 + \tilde{B}_0 \\
\tilde{V}_{\eta\eta} &= \alpha^2\tilde{V}_2 + \alpha\tilde{V}_1 + \tilde{V}_0
\end{aligned} \tag{38}$$

Then Eq. (36) is now written as

$$\begin{aligned}
&\alpha^2\left(\tilde{D}_2\psi + \tilde{B}_2\frac{\partial\psi}{\partial\eta} - \tilde{V}_2\frac{\partial^2\psi}{\partial\eta^2}\right) + \alpha\left(\tilde{D}_1\psi + \tilde{B}_1\frac{\partial\psi}{\partial\eta} - \tilde{V}_1\frac{\partial^2\psi}{\partial\eta^2}\right) \\
&+\left(\tilde{D}_0\psi + \tilde{B}_0\frac{\partial\psi}{\partial\eta} - \tilde{V}_0\frac{\partial^2\psi}{\partial\eta^2}\right) = 0
\end{aligned} \tag{39}$$

With similar discretization given in Eqs. (29) – (33), Eq. (39) can be put into

$$\alpha^2 H_2\Phi + \alpha H_1\Phi + H_0\Phi = 0 \tag{40}$$

where $\Phi = (\psi_{i,2}, \psi_{i,3}, \psi_{i,4} \cdots\cdots \psi_{i,JM-2}, \psi_{i,JM-1})^T$

This can be solved by reformulating it into the following manner [12] for which eigenvalue solver can be used.

$$\left(\alpha\begin{bmatrix} H_2 & 0 \\ 0 & I \end{bmatrix} + \begin{bmatrix} H_1 & H_0 \\ -I & 0 \end{bmatrix}\right)\begin{pmatrix} \alpha\Phi \\ \Phi \end{pmatrix} = \begin{pmatrix} 0 \\ 0 \end{pmatrix} \tag{41}$$

In order to test this procedure, two-dimensional and quasi-3D disturbances in supersonic and low subsonic flat plate flows have been considered. The first test is the case of $M=1.5, \beta=0.0, F=40, R_0=800, T_{stag}=311K$, where M is the Mach number of free stream, F is the non-dimensional frequency defined by $F=10^6(\omega^* \nu^* / u_\infty^{*2}) = 10^6(\omega / R_0)$, and T_{stag} is the stagnation temperature of the free stream.

As the Mach number increases, the critical layer, where the amplitudes of disturbances reach their maxima, moves away from the wall towards the edge of the boundary layer. The grid distributions suitable at certain Mach number must be chosen carefully. To catch unstable modes correctly, the grids need to be clustered in the critical layer. If there are equal-space grids in the general computational coordinate η direction, the clustered physical grid coordinates have the following form[13],

$$y_j = \frac{a\eta_j/\eta_{JM}}{b-\eta_j/\eta_{JM}} \quad (j=1,2,3,\cdots JM) \tag{42}$$

where j is the grid index of the normal direction from the wall, JM is the maximum grid number in that direction. Here $b=1+a/y_{max}$. Here y_{max} is the location where free-stream boundary conditions are satisfied and a is a scaling parameter chosen to optimize the accuracy of the calculation. Here use $a = y_{max} y_i/(y_{max}-2y_i)$ which puts half the node points used for discretization between $y=0$ and $y=y_i$. We take y_i to be 1.5 times non-dimensional displacement thickness at the starting point. During the whole calculations, we take y_{max} to be 100 and use 100 grid points in the wall normal direction.

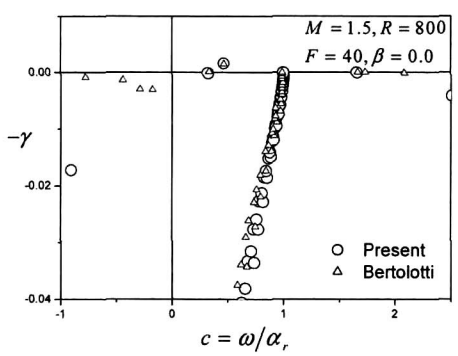

Fig. 1. Spectrum of eigenvalues, spatial growth, parallel flow, 2D disturbance

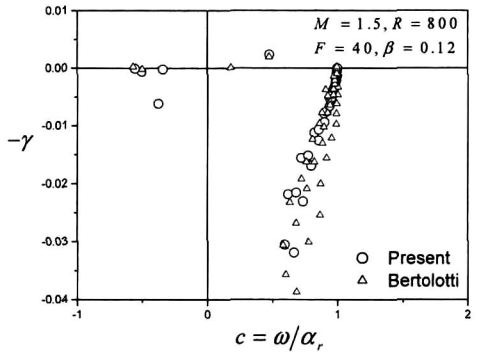

Fig. 2. Spectrum of eigenvalues, spatial growth, parallel flow, 3D disturbance

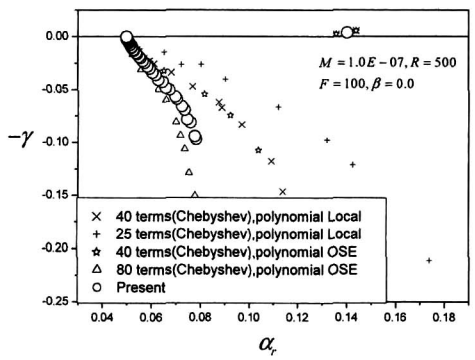

Fig. 3. Spectrum of spatial eigenvalues .Blasius boundary layer, results from PSE local procedure and from Orr-Sommerfeld equations

The real and the imaginary part of eigenvalue α are α_r and γ, respectively. The negative of γ denotes the growth rate. The eigenvalue spectrum obtained is shown in Fig. 1. The disturbance with $-\gamma$ greater than zero is unstable. From Fig. 1, we see that the spectral from the present finite difference method is in good agreement with that from the spectral method given by Bertolotti [14]. Next we increase the spanwise wave number to 0.12 and solve Eq. (41) with other parameters unchanged. The results are presented in Fig. 2. The comparison with Bertolotti's data shows that the present method works well in this case too.

To simulate incompressible flat flow case, a small Mach number is taken. The calculation is performed for the case of $M = 1.0E-07$, $\beta = 0.0$, $F = 100$, $R_0 = 1500$, $T_{stag} = 1100K$. Fig. 3 compares the present spectrum together with the spectrum of the Orr-Sommerfeld equations (OSE) and that of the local formulations in which nonparallel effect invoked. Fig. 3 indicates that the present method gives the data very close to the Chebyshev method using 80 terms. This demonstrates that the present finite difference method is indeed a good alternative for spectral method. To be more specific, we pick out the unstable modes from Figs. 1-3 and compare those with Bertolotti's data.

(1) Test 1

$M = 1.5, \beta = 0.0, F = 40, R = 800, T_{stag} = 311K$

Bertolotti: $-\gamma = 0.00149166, \omega/\alpha_r = 0.46859732$

Present: $-\gamma = 0.00148996, \omega/\alpha_r = 0.46758789$

(2) Test 2

$M = 1.5, \beta = 0.12, F = 40, R = 800, T_{stag} = 311K$

Bertolotti: $-\gamma = 0.00201235, \omega/\alpha_r = 0.47794939$

Present: $-\gamma = 0.00209985, \omega/\alpha_r = 0.47257210$

(3) Test 3

$M = 1.0E-07, \beta = 0.0, F = 100, R = 1500, T_{stag} = 1100K$

Bertolotti: $-\gamma = 0.00366564, \alpha_r = 0.14022725$

Present: $-\gamma = 0.00362831, \alpha_r = 0.14009549$

The above data clearly shows that the present method is capable of picking up unstable modes accurately and thus generates good initial conditions for the PSE calculation.

Mean Flow Computations

To validate the present PSE code in general curvilinear coordinate system, the insulated flat plate flow is first tested. The mean flow is obtained by the coupled laminar boundary layer code using the Falkner-Skan transformation[15], which is suitable for the stability calculation. The code used here has been modified to calculate the flows with largely varying properties. The dependence of the specific heat c_p, the viscosity μ, and the conductivity κ on temperature is approximated with a fourth-order polynomial given by least squares interpolation of experimental data between the temperature of 100K and 1600K. The coefficients for the fourth-order degree polynomial expansion in temperature for c_p, μ, and κ are given in Table 1, valid for 100K<T<1600K[14]. One can anticipate that in supersonic flows a change in growth rate of ten percent or more due to the thermodynamic approximations could easily pollute the measurements of nonparallel effects.

Table 1. Values of the coefficients used in the polynomial approximation

$$Value = c_0 + c_1 T + c_2 T^2 + c_3 T^3 + c_4 T^4$$

c_n	$c_p(J/kg-K)$	$\mu(N-s/m^2)$	$\kappa(W/m-K)$
0	1.058183878E+03	−1.561632014E−07	−1.305884703E−03
1	−4.524547049E−01	7.957989891E−08	1.099134492E−04
2	1.141345435E−03	−6.930149679E−11	−6.846979087E−08
3	−7.957390422E−07	4.068157752E−14	3.327083322E−11
4	1.910858151E−10	−9.182486030E−18	−5.397866355E−15

Thus it is crucial to get an accurate value of properties especially at high Mach number for the stability analysis.

The large effect of properties can be found by comparing the results obtained under the following two conditions:

(a) c_p is held constant at its value at $273\,K$ while the viscosity μ and the conductivity κ vary polynomially

(b) All the coefficients vary polynomially.

The results are shown in Figs. 4 and 5. Fig. 5 indicates that the effect of property variation gets more important as the free stream Mach number increases.

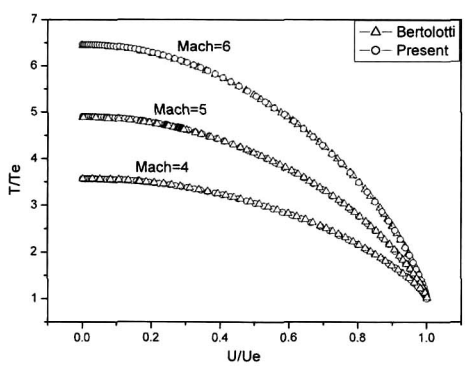

Fig. 4. Mean flow calculation at different Mach number based on variable specific heat, viscosity and conductivity

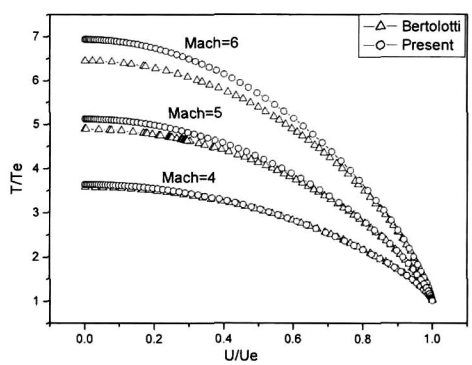

Fig. 5. Mean flow calculation at different Mach number based on constant specific heat, variable viscosity and conductivity

Code validations

For three−dimensional disturbances, we introduce the parameter b which is proportional to the dimensional wave number in spanwise direction defined by

$$b = \beta \cdot 10^3 / R_0 \tag{43}$$

The division by R_0 makes b independent of the reference length. We comment here that the dimensional spanwise wave number remains constant as the TS wave is convected downstream.

The first test is carried out for compressible flat plate flow with two−dimensional disturbances. The Mach number of free stream is taken to be 1.6, the non−dimensional

frequency F is 40 and the stagnation temperature of the free stream is 311 K. The comparison of growth rates obtained by the present code and by the multiple scales method reported by El-Hady & Nayfeh[16] is shown in Fig. 6. In abscissa, R is the Reynolds number ($R = \sqrt{u_\infty^* x^* / \nu_\infty^*}$). Fig. 6 shows that the growth rate of the present PSE code is in good agreement with that of the multiple scales method. We find that the growth rate

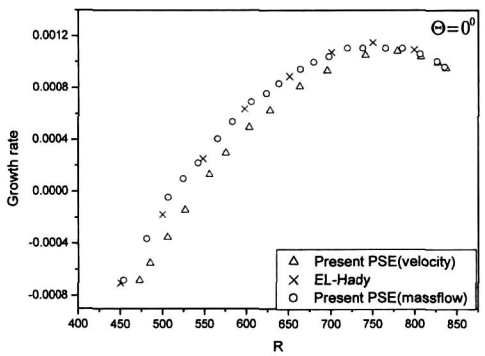

Fig. 6. Growth rates & R at $M = 1.6, F = 40$, $b = 0, T_{stag} = 311K$ .Comparison with multiple scales data of EL-Hady, Θ denotes wave angle

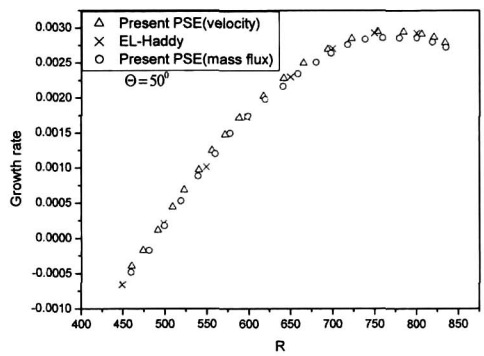

Fig. 7. Growth rates & R at $M = 1.6, F = 40$, $b = 0.10, T_{stag} = 311K$ .Comparison with multiple scales data of EL-Hady, Θ denotes wave angle

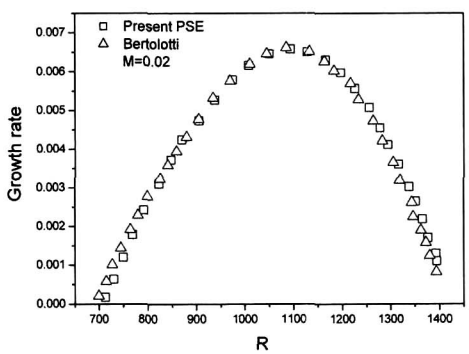

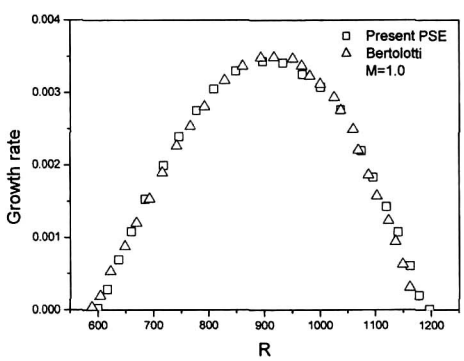

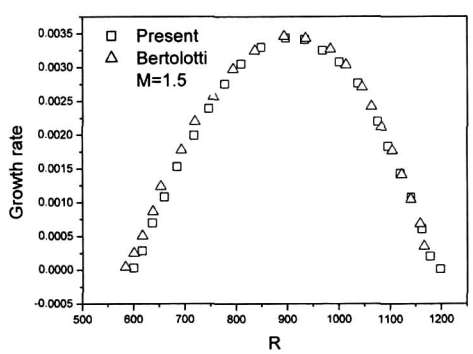

Fig. 8. Growth rates & R at $F = 40, b = 0, T_{stag} = 311K$ for various Mach numbers using present PSE code with a comparison with Bertolotti's nonparallel results

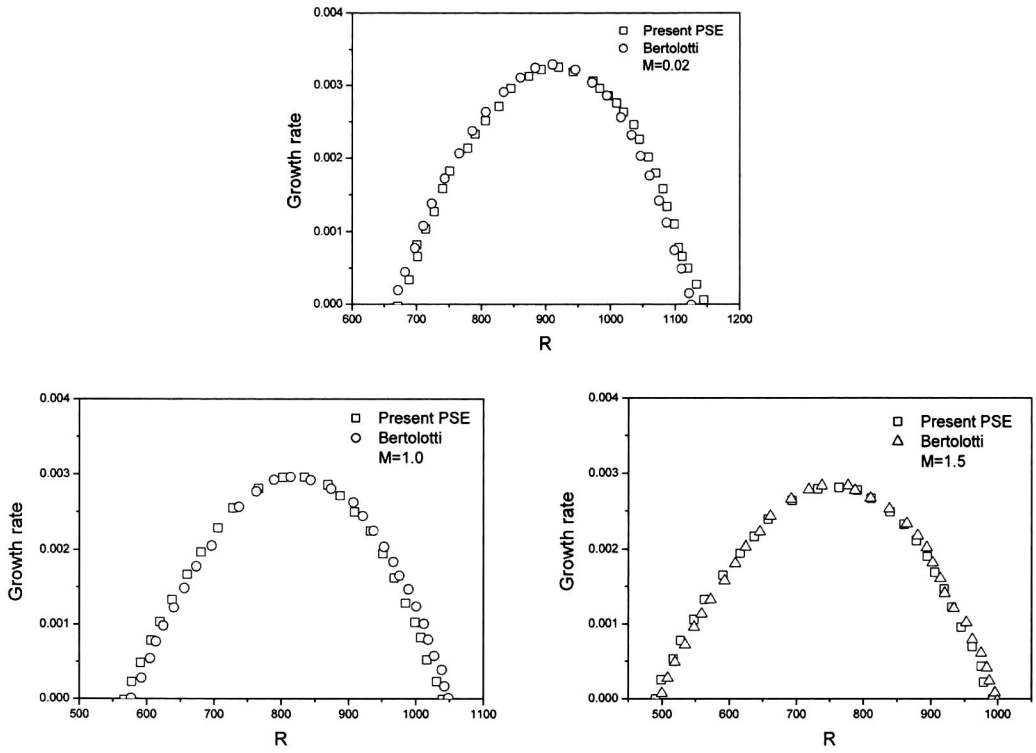

Fig. 9. Growth rates & R at $F = 40, b = 0.15, T_{stag} = 311K$ for various Mach numbers. Parallel and nonparallel basic-flow results

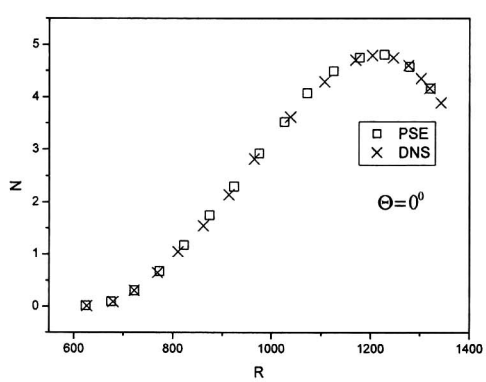

Fig. 10. The variation of amplification factor of 2D disturbances with streamwise position at $F = 50, T_{stag} = 311K, M = 10^{-6}$ comparing DNS

obtained from maximum mass flux is in better agreement than that from maximum velocity for two dimensional disturbances. Next, we increase the non-dimensional spanwise wave number b to 0.1 with other parameters unchanged; the quasi-3D disturbance evolvement is shown in Fig. 7. The comparison clearly indicates that the present PSE code produces very good results for 3D disturbances.

We have a series of tests at different Mach number ranging from 0.02 to 1.5 at $F = 40, T_{stag} = 311K$. First, we concentrate on 2D disturbance ($b = 0$). The temperature

of the free stream is held constant at 206 K, and the plate is insulated. All the thermodynamic coefficients are approximated by fourth-order polynomial. The results obtained from the present PSE code are compared with the nonparallel results of Bertolotti [14]. Fig. 8 displays that the data from the present finite difference method is in good agreement with those from the spectral method at subsonic and supersonic flows. Then we increase the spanwise wave number to $b = 0.15$ with other parameters unchanged. The growth rates obtained from the present method at different Mach number are shown in Fig. 9. We see that the comparison with the nonparallel results of Bertolotti indicates that present code is rather accurate.

The third test is done for incompressible flat plate flow for two-dimensional disturbances. The flow conditions are: $M = 10^{-6}$, $F = 50$, $T_{stag} = 311K$. The amplification factors denoted by N obtained from present PSE code and by DNS[14] are presented in Fig. 10. We see that the agreement with DNS data is remarkably good.

Conclusions

Parabolized stability equations in curvilinear coordinate system are derived. A highly accurate finite difference PSE code has been developed at a general curvilinear coordinate system using an implicit marching procedure. Two dimensional and three dimensional disturbances at compressible/incompressible flat plate flows are tested. The results of the present computation show good agreement with multiple scale method and DNS method. Comparison with spectral method for 2D/3D disturbances at different Mach number is also carried out and the result again demonstrates the accuracy for the present finite difference scheme.

Acknowledgment

This research was supported by the Flight Vehicle Research Center at Seoul National University under the sponsorship of Ministry of Defense, Korea. The first author also deeply acknowledges the foreign student scholarship from the Korea Research Foundation.

References

1. D. Arnal, Description and prediction of transition two dimensional incompressible flows. In special Course on Stability and Transition of Laminar Flows, AGARD Report 709, 1984.

2. D. Arnal, Boundary layer transition: Predictions based on linear theory. In special Course on Progress in Transition Modeling. AGARD reports, 793, 1994.

3. V. Esfahanian and K. Hejranfar, Linear and Nonlinear PSE for Stability Analysis of the Blasius Boundary Layer Using Compact Scheme. Journal of Fluids Engineering. ASME. September 2001, Vol. 123.

4. Th. Herbert and F. P. Bertolotti, Stability analysis of nonparallel boundary layers. J. Bull. AM. Phys. Soc., 32, pp. 2079, 1987.

5. S. Hu and X. Zhong, Nonparallel stability Analysis of Compressible Boundary Layer using 3-D PSE. AIAA-1999-0813.

6. C. L. Chang and M. R. Malik, Compressible Stability of Growing Boundary Layers Using Parabolized Stability Equations. AIAA-1991-1636.

7. Th. Herbert and M. V. Morkovin, Dialogue on bridging some gaps in stability and transition research. Laminar-Turbulent Transition. (Ed) R.Eppler and H. Fasel, Springer-Verlag, 1980.

8. L. M. Mack, 1977. Transition prediction and linear stability theory. In Laminar-Turbulent Transition. AGARD CP 224.

9. F. P. Bertolotti, Compressible Boundary Layer Stability analyzed with the PSE equations. AIAA-1991-1637.

10. Th. Herbert, Parabolized stability equations. Annual Review of Fluid Mechanics. Vol. 29, January, 1997

11. M. R. Malik, Hypersonic Flight Transition Data Analysis Using Parabolized Stability Equations with Chemistry Effects. Journal of Spacecraft and Rockets. Vol. 40, NO. 3, May-June 2003.

12. F. Tisseur and K. Meerbergen, The Quadratic Eigenvalue Problem. SIAM REVIEW. Vol. 43, No. 2, 2001.

13. M. R. Malik, Numerical methods for hypersonic boundary layer stability. Journal of computational physics 86, 1990.

14. F. P. Bertolotti, Linear and nonlinear stability of boundary layers with streamwise varying properties. Ph D dissertation. The Ohio State University, 1991.

15. T. Cebeci and P. Bradshaw, Physical and Computational Aspects of Convective Heat Transfer. Springer-Verlag. New York.

16. El-Hady N. M. and Nayfeh A. H., Nonparallel stability of compressible boundary layer flows. AIAA-1980-0277.

Appendix A : Coefficients of the disturbance equation

The coefficients of Eq. (7) are as follows. The symbol l_j is introduced for convenience with $l_j = j + \lambda/\mu$.

$$\Gamma = \begin{bmatrix} \Gamma_{11} & 0 & 0 & 0 & \Gamma_{15} \\ 0 & \Gamma_{22} & 0 & 0 & 0 \\ 0 & 0 & \Gamma_{33} & 0 & 0 \\ 0 & 0 & 0 & \Gamma_{44} & 0 \\ \Gamma_{51} & 0 & 0 & 0 & \Gamma_{55} \end{bmatrix}; \quad A = \begin{bmatrix} A_{11} & A_{12} & 0 & 0 & A_{15} \\ A_{21} & A_{22} & A_{23} & A_{24} & A_{25} \\ 0 & A_{32} & A_{33} & 0 & A_{35} \\ 0 & A_{42} & 0 & A_{44} & A_{45} \\ A_{51} & A_{52} & A_{53} & A_{54} & A_{55} \end{bmatrix};$$

$$B = \begin{bmatrix} B_{11} & 0 & B_{13} & 0 & B_{15} \\ 0 & B_{22} & B_{23} & 0 & B_{25} \\ B_{31} & B_{32} & B_{33} & B_{34} & B_{35} \\ 0 & 0 & B_{43} & B_{44} & B_{45} \\ B_{51} & B_{52} & B_{53} & B_{54} & B_{55} \end{bmatrix}; \quad C = \begin{bmatrix} C_{11} & 0 & 0 & C_{14} & C_{15} \\ 0 & C_{22} & 0 & C_{24} & C_{25} \\ 0 & 0 & C_{33} & C_{34} & C_{35} \\ C_{41} & C_{42} & C_{43} & C_{44} & C_{45} \\ C_{51} & C_{52} & C_{53} & C_{54} & C_{55} \end{bmatrix};$$

$$D = \begin{bmatrix} D_{11} & D_{12} & D_{13} & D_{14} & D_{15} \\ D_{21} & D_{22} & D_{23} & D_{24} & D_{25} \\ D_{31} & D_{32} & D_{33} & D_{34} & D_{35} \\ D_{41} & D_{42} & D_{43} & D_{44} & D_{45} \\ D_{51} & D_{52} & D_{53} & D_{54} & D_{55} \end{bmatrix}; \quad V_{xx} = \begin{bmatrix} 0 & 0 & 0 & 0 & 0 \\ 0 & V_{xx}^{22} & 0 & 0 & 0 \\ 0 & 0 & V_{xx}^{33} & 0 & 0 \\ 0 & 0 & 0 & V_{xx}^{44} & 0 \\ 0 & 0 & 0 & 0 & V_{xx}^{55} \end{bmatrix};$$

$$V_{yy} = \begin{bmatrix} 0 & 0 & 0 & 0 & 0 \\ 0 & V_{yy}^{22} & 0 & 0 & 0 \\ 0 & 0 & V_{yy}^{33} & 0 & 0 \\ 0 & 0 & 0 & V_{yy}^{44} & 0 \\ 0 & 0 & 0 & 0 & V_{yy}^{55} \end{bmatrix}; \quad V_{zz} = \begin{bmatrix} 0 & 0 & 0 & 0 & 0 \\ 0 & V_{zz}^{22} & 0 & 0 & 0 \\ 0 & 0 & V_{zz}^{33} & 0 & 0 \\ 0 & 0 & 0 & V_{zz}^{44} & 0 \\ 0 & 0 & 0 & 0 & V_{zz}^{55} \end{bmatrix};$$

$$V_{xy} = \begin{bmatrix} 0 & 0 & 0 & 0 & 0 \\ 0 & 0 & V_{xy}^{23} & 0 & 0 \\ 0 & V_{xy}^{32} & 0 & 0 & 0 \\ 0 & 0 & 0 & 0 & 0 \\ 0 & 0 & 0 & 0 & 0 \end{bmatrix}; \quad V_{xz} = \begin{bmatrix} 0 & 0 & 0 & 0 & 0 \\ 0 & 0 & 0 & V_{xz}^{24} & 0 \\ 0 & 0 & 0 & 0 & 0 \\ 0 & V_{xz}^{42} & 0 & 0 & 0 \\ 0 & 0 & 0 & 0 & 0 \end{bmatrix};$$

$$V_{yz}=\begin{bmatrix}0&0&0&0&0\\0&0&0&0&0\\0&0&0&V_{yz}^{34}&0\\0&0&V_{yz}^{43}&0&0\\0&0&0&0&0\end{bmatrix};$$

$$\Gamma_{11}=\frac{\gamma M^2}{T},\quad \Gamma_{15}=-\frac{\rho}{T},\quad \Gamma_{51}=-(\gamma-1)M^2,\quad \Gamma_{22}=\Gamma_{33}=\Gamma_{44}=\Gamma_{55}=\rho,$$

$$A_{11}=\gamma M^2\frac{U}{T},\quad A_{12}=\rho,\quad A_{15}=-U\frac{\rho}{T},\quad A_{21}=1,\quad A_{22}=\rho U-\frac{1}{R}\frac{d\mu}{dT}\frac{\partial T}{\partial x}l_2,$$

$$A_{23}=-\frac{1}{R}\frac{d\mu}{dT}\frac{\partial T}{\partial y},\quad A_{24}=-\frac{1}{R}\frac{d\mu}{dT}\frac{\partial T}{\partial z},\quad A_{25}=-\frac{1}{R}\frac{d\mu}{dT}\left(l_2\frac{\partial U}{\partial x}+l_0\frac{\partial V}{\partial y}+l_0\frac{\partial W}{\partial z}\right),$$

$$A_{32}=-\frac{l_0}{R}\frac{d\mu}{dT}\frac{\partial T}{\partial y},\quad A_{33}=\rho U-\frac{1}{R}\frac{d\mu}{dT}\frac{\partial T}{\partial x},\quad A_{35}=-\frac{1}{R}\frac{d\mu}{dT}\left(\frac{\partial U}{\partial y}+\frac{\partial V}{\partial x}\right),$$

$$A_{42}=-\frac{1}{R}\frac{d\mu}{dT}\frac{\partial T}{\partial z}l_0,\quad A_{44}=\rho U-\frac{1}{R}\frac{d\mu}{dT}\frac{\partial T}{\partial x},\quad A_{45}=-\frac{1}{R}\frac{d\mu}{dT}\left(\frac{\partial W}{\partial x}+\frac{\partial U}{\partial z}\right),$$

$$A_{51}=-(\gamma-1)M^2U,\quad A_{52}=-2(\gamma-1)M^2\frac{\mu}{R}\left(l_2\frac{\partial U}{\partial x}+l_0\frac{\partial V}{\partial y}+l_0\frac{\partial W}{\partial z}\right),$$

$$A_{53}=-2(\gamma-1)M^2\frac{\mu}{R}\left(\frac{\partial U}{\partial y}+\frac{\partial V}{\partial x}\right),$$

$$A_{54}=-2(\gamma-1)M^2\frac{\mu}{R}\left(\frac{\partial U}{\partial z}+\frac{\partial W}{\partial x}\right),\quad A_{55}=\rho U-\frac{2}{R\,\mathrm{Pr}}\frac{dk}{dT}\frac{\partial T}{\partial x},$$

$$B_{11}=\gamma M^2\frac{V}{T},\quad B_{13}=\rho,\quad B_{15}=-V\frac{\rho}{T},\quad B_{22}=\rho V-\frac{1}{R}\frac{d\mu}{dT}\frac{\partial T}{\partial y},\quad B_{23}=-\frac{1}{R}\frac{d\mu}{dT}\frac{\partial T}{\partial x}l_0,$$

$$B_{25}=-\frac{1}{R}\frac{d\mu}{dT}\left(\frac{\partial U}{\partial y}+\frac{\partial V}{\partial x}\right),\quad B_{31}=1,\quad B_{32}=-\frac{1}{R}\frac{d\mu}{dT}\frac{\partial T}{\partial x},\quad B_{33}=\rho V-\frac{l_2}{R}\frac{d\mu}{dT}\frac{\partial T}{\partial y},$$

$$B_{34}=-\frac{1}{R}\frac{d\mu}{dT}\frac{\partial T}{\partial z},\quad B_{35}=-\frac{1}{R}\frac{d\mu}{dT}\left(l_0\frac{\partial U}{\partial x}+l_2\frac{\partial V}{\partial y}+l_0\frac{\partial W}{\partial z}\right),\quad B_{43}=-\frac{1}{R}\frac{d\mu}{dT}\frac{\partial T}{\partial z}l_0,$$

$$B_{44}=\rho V-\frac{1}{R}\frac{d\mu}{dT}\frac{\partial T}{\partial y},\quad B_{45}=-\frac{1}{R}\frac{d\mu}{dT}\left(\frac{\partial V}{\partial z}+\frac{\partial W}{\partial y}\right),\quad B_{51}=-(\gamma-1)M^2V,$$

$$B_{52}=-2(\gamma-1)M^2\frac{\mu}{R}\left(\frac{\partial U}{\partial y}+\frac{\partial V}{\partial x}\right),\quad B_{53}=-2(\gamma-1)M^2\frac{\mu}{R}\left(l_0\frac{\partial U}{\partial x}+l_2\frac{\partial V}{\partial y}+l_0\frac{\partial W}{\partial z}\right),$$

$$B_{54}=-2(\gamma-1)M^2\frac{\mu}{R}\left(\frac{\partial V}{\partial z}+\frac{\partial W}{\partial y}\right),\quad B_{55}=\rho V-\frac{2}{R\,\mathrm{Pr}}\frac{dk}{dT}\frac{\partial T}{\partial y},\quad C_{11}=\gamma M^2\frac{W}{T},$$

$$C_{14}=\rho,\quad C_{15}=-W\frac{\rho}{T},\quad C_{22}=\rho W-\frac{1}{R}\frac{d\mu}{dT}\frac{\partial T}{\partial z},\quad C_{24}=-\frac{1}{R}\frac{d\mu}{dT}\frac{\partial T}{\partial x}l_0,$$

$$C_{25}=-\frac{1}{R}\frac{d\mu}{dT}\left(\frac{\partial W}{\partial x}+\frac{\partial U}{\partial z}\right),\quad C_{33}=\rho W-\frac{1}{R}\frac{d\mu}{dT}\frac{\partial T}{\partial z},\quad C_{34}=-\frac{l_0}{R}\frac{d\mu}{dT}\frac{\partial T}{\partial y},$$

$$C_{35}=-\frac{1}{R}\frac{d\mu}{dT}\left(\frac{\partial V}{\partial z}+\frac{\partial W}{\partial y}\right),\quad C_{41}=1,\quad C_{42}=-\frac{1}{R}\frac{d\mu}{dT}\frac{\partial T}{\partial x},\quad C_{43}=-\frac{1}{R}\frac{d\mu}{dT}\frac{\partial T}{\partial y},$$

$$C_{44}=\rho W-\frac{1}{R}\frac{d\mu}{dT}\frac{\partial T}{\partial z}l_2,\quad C_{45}=-\frac{1}{R}\frac{d\mu}{dT}(l_0\frac{\partial U}{\partial x}+l_0\frac{\partial V}{\partial y}+l_2\frac{\partial W}{\partial z}),$$

$$C_{51}=-(\gamma-1)M^2W,\quad C_{52}=-2(\gamma-1)M^2\frac{\mu}{R}(\frac{\partial U}{\partial z}+\frac{\partial W}{\partial x}),$$

$$C_{53}=-2(\gamma-1)M^2\frac{\mu}{R}(\frac{\partial V}{\partial z}+\frac{\partial W}{\partial y}),\quad C_{54}=-2(\gamma-1)M^2\frac{\mu}{R}(l_0\frac{\partial U}{\partial x}+l_0\frac{\partial V}{\partial y}+l_2\frac{\partial W}{\partial z}),$$

$$C_{55}=\rho W-\frac{2}{R\,\mathrm{Pr}}\frac{dk}{dT}\frac{\partial T}{\partial z},\quad D_{11}=\frac{\gamma M^2}{T}(\frac{\partial U}{\partial x}+\frac{\partial V}{\partial y}+\frac{\partial W}{\partial z})-\frac{\gamma M^2}{T^2}(U\frac{\partial T}{\partial x}+V\frac{\partial T}{\partial y}+W\frac{\partial T}{\partial z}),$$

$$D_{12}=\frac{\partial\rho}{\partial x},\quad D_{13}=\frac{\partial\rho}{\partial y},\quad D_{14}=\frac{\partial\rho}{\partial z},$$

$$D_{15}=\frac{\rho}{T^2}(U\frac{\partial T}{\partial x}+V\frac{\partial T}{\partial y}+W\frac{\partial T}{\partial z})-\frac{1}{T}(U\frac{\partial\rho}{\partial x}+V\frac{\partial\rho}{\partial y}+W\frac{\partial\rho}{\partial z})-\frac{\rho}{T}(\frac{\partial U}{\partial x}+\frac{\partial V}{\partial y}+\frac{\partial W}{\partial z}),$$

$$D_{21}=\frac{\gamma M^2}{T}(U\frac{\partial U}{\partial x}+V\frac{\partial U}{\partial y}+W\frac{\partial U}{\partial z}),\quad D_{22}=\rho\frac{\partial U}{\partial x},\quad D_{23}=\rho\frac{\partial U}{\partial y},\quad D_{24}=\rho\frac{\partial U}{\partial z},$$

$$D_{25}=-\frac{\rho}{T}(U\frac{\partial U}{\partial x}+V\frac{\partial U}{\partial y}+W\frac{\partial U}{\partial z})-\frac{1}{R}\frac{d\mu}{dT}(l_2\frac{\partial^2U}{\partial x^2}+l_0\frac{\partial^2V}{\partial y\partial x}+l_0\frac{\partial^2W}{\partial z\partial x})$$
$$-\frac{1}{R}\frac{d^2\mu}{dT^2}\frac{\partial T}{\partial x}(l_2\frac{\partial U}{\partial x}+l_0\frac{\partial V}{\partial y}+l_0\frac{\partial W}{\partial z})-\frac{1}{R}\frac{d\mu}{dT}(\frac{\partial^2U}{\partial y\partial y}+\frac{\partial^2V}{\partial x\partial y})$$
$$-\frac{1}{R}\frac{d^2\mu}{dT^2}\frac{\partial T}{\partial y}(\frac{\partial U}{\partial y}+\frac{\partial V}{\partial x})-\frac{1}{R}\frac{d\mu}{dT}(\frac{\partial^2W}{\partial x\partial z}+\frac{\partial^2U}{\partial z\partial z})-\frac{1}{R}\frac{d^2\mu}{dT^2}\frac{\partial T}{\partial z}(\frac{\partial W}{\partial x}+\frac{\partial U}{\partial z}),$$

$$D_{31}=\frac{\gamma M^2}{T}(U\frac{\partial V}{\partial x}+V\frac{\partial V}{\partial y}+W\frac{\partial V}{\partial z}),\quad D_{32}=\rho\frac{\partial V}{\partial x},\quad D_{33}=\rho\frac{\partial V}{\partial y},\quad D_{34}=\rho\frac{\partial V}{\partial z},$$

$$D_{35}=-\frac{\rho}{T}(U\frac{\partial V}{\partial x}+V\frac{\partial V}{\partial y}+W\frac{\partial V}{\partial z})-\frac{1}{R}\frac{d\mu}{dT}(\frac{\partial^2U}{\partial y\partial x}+\frac{\partial^2V}{\partial x\partial x})-\frac{1}{R}\frac{d^2\mu}{dT^2}\frac{\partial T}{\partial x}(\frac{\partial U}{\partial y}+\frac{\partial V}{\partial x})$$
$$-\frac{1}{R}\frac{d\mu}{dT}(l_0\frac{\partial^2U}{\partial x\partial y}+l_2\frac{\partial^2V}{\partial y\partial y}+l_0\frac{\partial^2W}{\partial z\partial y})-\frac{1}{R}\frac{d^2\mu}{dT^2}\frac{\partial T}{\partial y}(l_0\frac{\partial U}{\partial x}+l_2\frac{\partial V}{\partial y}+l_0\frac{\partial W}{\partial z})$$
$$-\frac{1}{R}\frac{d\mu}{dT}(\frac{\partial^2V}{\partial z\partial z}+\frac{\partial^2W}{\partial y\partial z})-\frac{1}{R}\frac{d^2\mu}{dT^2}\frac{\partial T}{\partial z}(\frac{\partial V}{\partial z}+\frac{\partial W}{\partial y}),$$

$$D_{41}=\frac{\gamma M^2}{T}(U\frac{\partial W}{\partial x}+V\frac{\partial W}{\partial y}+W\frac{\partial W}{\partial z}),\quad D_{42}=\rho\frac{\partial W}{\partial x},\quad D_{43}=\rho\frac{\partial W}{\partial y},\quad D_{44}=\rho\frac{\partial W}{\partial z},$$

$$D_{45}=-\frac{\rho}{T}(U\frac{\partial W}{\partial x}+V\frac{\partial W}{\partial y}+W\frac{\partial W}{\partial z})-\frac{1}{R}\frac{d\mu}{dT}(\frac{\partial^2W}{\partial x\partial x}+\frac{\partial^2U}{\partial x\partial z})-\frac{1}{R}\frac{d^2\mu}{dT^2}\frac{\partial T}{\partial x}(\frac{\partial W}{\partial x}+\frac{\partial U}{\partial z})$$
$$-\frac{1}{R}\frac{d\mu}{dT}(\frac{\partial^2V}{\partial y\partial z}+\frac{\partial^2W}{\partial y\partial y})-\frac{1}{R}\frac{d^2\mu}{dT^2}\frac{\partial T}{\partial y}(\frac{\partial V}{\partial z}+\frac{\partial W}{\partial y})-\frac{1}{R}\frac{d^2\mu}{dT^2}\frac{\partial T}{\partial z}(l_0\frac{\partial U}{\partial x}+l_0\frac{\partial V}{\partial y}+l_2\frac{\partial W}{\partial z})$$
$$-\frac{1}{R}\frac{d\mu}{dT}(l_0\frac{\partial^2U}{\partial x\partial z}+l_0\frac{\partial^2V}{\partial y\partial z}+l_2\frac{\partial^2W}{\partial z\partial z}),$$

$$D_{51}=\frac{\gamma M^2}{T}(U\frac{\partial T}{\partial x}+V\frac{\partial T}{\partial y}+W\frac{\partial T}{\partial z}),\quad D_{52}=\rho\frac{\partial T}{\partial x}-(\gamma-1)M^2\frac{\partial P}{\partial x},$$

$$D_{53}=\rho\frac{\partial T}{\partial y}-(\gamma-1)M^2\frac{\partial P}{\partial y},\quad D_{54}=\rho\frac{\partial T}{\partial z}-(\gamma-1)M^2\frac{\partial P}{\partial z},$$

$$D_{55} = -\frac{\rho}{T}(U\frac{\partial T}{\partial x}+V\frac{\partial T}{\partial y}+W\frac{\partial T}{\partial z})-\frac{1}{R\,\mathrm{Pr}}\frac{dk}{dT}(\frac{\partial^2 T}{\partial x^2}+\frac{\partial^2 T}{\partial y^2}+\frac{\partial^2 T}{\partial z^2})$$
$$-\frac{1}{R\,\mathrm{Pr}}\frac{d^2k}{dT^2}\left[(\frac{\partial T}{\partial x})^2+(\frac{\partial T}{\partial y})^2+(\frac{\partial T}{\partial z})^2\right]-(\gamma-1)M^2\frac{1}{R}\frac{d\mu}{dT}\left\{l_2\left[(\frac{\partial U}{\partial x})^2+(\frac{\partial V}{\partial y})^2+(\frac{\partial W}{\partial z})^2\right]\right.$$
$$\left.+2l_0(\frac{\partial U}{\partial x}\frac{\partial V}{\partial y}+\frac{\partial U}{\partial x}\frac{\partial W}{\partial z}+\frac{\partial V}{\partial y}\frac{\partial W}{\partial z})+(\frac{\partial U}{\partial y}+\frac{\partial V}{\partial x})^2+(\frac{\partial V}{\partial z}+\frac{\partial W}{\partial y})^2+(\frac{\partial U}{\partial z}+\frac{\partial W}{\partial x})^2\right\}$$

$$V_{xx}^{22}=V_{yy}^{33}=V_{zz}^{44}=\frac{\mu}{R}l_2\quad,\quad V_{xx}^{33}=V_{xx}^{44}=V_{yy}^{22}=V_{yy}^{44}=V_{zz}^{22}=V_{zz}^{33}=\frac{\mu}{R}$$

$$V_{xx}^{55}=V_{yy}^{55}=V_{zz}^{55}=\frac{k}{R\,\mathrm{Pr}}\quad,\quad V_{xy}^{23}=V_{xy}^{32}=V_{xz}^{24}=V_{xz}^{42}=V_{yz}^{34}=V_{yz}^{43}=\frac{\mu}{R}l_0+\frac{\mu}{R}$$

Appendix B: Coefficients Matrices Relations

The relation between $\overline{\Gamma}, \overline{A}, \overline{B}, \overline{C}, \overline{D}, \overline{V}_{xx}, \overline{V}_{yy}, \overline{V}_{zz}, \overline{V}_{xy}, \overline{V}_{xz}, \overline{V}_{yz}$ of Eq. (9) and $\Gamma, A, B, C, D, V_{xx}, V_{yy}, V_{zz}, V_{xy}, V_{xz}, V_{yz}$ of Eq. (7) are as follows

$$\overline{\Gamma}(\xi, \eta, \zeta) = \Gamma(x, y, z)$$

$$\overline{A} = (A\xi_x + B\xi_y + C\xi_z) - (V_{xx}\frac{\partial^2\xi}{\partial x^2} + V_{yy}\frac{\partial^2\xi}{\partial y^2} + V_{zz}\frac{\partial^2\xi}{\partial z^2} + V_{xy}\frac{\partial^2\xi}{\partial x\partial y} + V_{yz}\frac{\partial^2\xi}{\partial z\partial y} + V_{xz}\frac{\partial^2\xi}{\partial z\partial x})$$

$$\overline{B} = (A\eta_x + B\eta_y + C\eta_z) - (V_{xx}\frac{\partial^2\eta}{\partial x^2} + V_{yy}\frac{\partial^2\eta}{\partial y^2} + V_{zz}\frac{\partial^2\eta}{\partial z^2} + V_{xy}\frac{\partial^2\eta}{\partial x\partial y} + V_{yz}\frac{\partial^2\eta}{\partial z\partial y} + V_{xz}\frac{\partial^2\eta}{\partial z\partial x})$$

$$\overline{C} = (A\zeta_x + B\zeta_y + C\zeta_z) - (V_{xx}\frac{\partial^2\zeta}{\partial x^2} + V_{yy}\frac{\partial^2\zeta}{\partial y^2} + V_{zz}\frac{\partial^2\zeta}{\partial z^2} + V_{xy}\frac{\partial^2\zeta}{\partial x\partial y} + V_{yz}\frac{\partial^2\zeta}{\partial z\partial y} + V_{xz}\frac{\partial^2\zeta}{\partial z\partial x})$$

$$\overline{D}(\xi, \eta, \zeta) = D(x, y, z)$$

$$\overline{V}_{\xi\xi} = V_{xx}\xi_x^2 + V_{yy}\xi_y^2 + V_{zz}\xi_z^2 + V_{xy}\xi_x\xi_y + V_{yz}\xi_z\xi_y + V_{xz}\xi_z\xi_x$$

$$\overline{V}_{\eta\eta} = V_{xx}\eta_x^2 + V_{yy}\eta_y^2 + V_{zz}\eta_z^2 + V_{xy}\eta_x\eta_y + V_{yz}\eta_z\eta_y + V_{xz}\eta_z\eta_x$$

$$\overline{V}_{\zeta\zeta} = V_{xx}\zeta_x^2 + V_{yy}\zeta_y^2 + V_{zz}\zeta_z^2 + V_{xy}\zeta_x\zeta_y + V_{yz}\zeta_z\zeta_y + V_{xz}\zeta_z\zeta_x$$

$$\overline{V}_{\eta\zeta} = 2V_{xx}\zeta_x\eta_x + 2V_{yy}\zeta_y\eta_y + 2V_{zz}\zeta_z\eta_z + V_{xy}(\zeta_x\eta_y + \eta_x\zeta_y) + V_{yz}(\zeta_z\eta_y + \eta_z\zeta_y) + V_{xz}(\zeta_z\eta_x + \eta_z\zeta_x)$$

$$\overline{V}_{\xi\zeta} = 2V_{xx}\zeta_x\xi_x + 2V_{yy}\zeta_y\xi_y + 2V_{zz}\zeta_z\xi_z + V_{xy}(\zeta_x\xi_y + \xi_x\zeta_y) + V_{yz}(\zeta_z\xi_y + \xi_z\zeta_y) + V_{xz}(\zeta_z\xi_x + \xi_z\zeta_x)$$

$$\overline{V}_{\xi\eta} = 2V_{xx}\eta_x\xi_x + 2V_{yy}\eta_y\xi_y + 2V_{zz}\eta_z\xi_z + V_{xy}(\eta_x\xi_y + \xi_x\eta_y) + V_{yz}(\eta_z\xi_y + \xi_z\eta_y) + V_{xz}(\eta_z\xi_x + \xi_z\eta_x)$$